Int. J. Electrochem. Sci., 11 **(2016)** 1482 - 1495

International Journal of
ELECTROCHEMICAL
SCIENCE
www.electrochemsci.org

Short Review

Review on Corrosion Behavior of Metallic Materials in Room Temperature Ionic Liquids

Bonita Dilasari[1], *Yeojin Jung*[1], *Jeongsoo Sohn*[2], *Sookyung Kim*[2,*], *Kyungjung Kwon*[1,*]

[1] Department of Energy & Mineral Resources Engineering, Sejong University, 209 Neungdong-ro, Gwangjin-gu, Seoul 05006, Republic of Korea
[2] Urban Mine Department, Korea Institute of Geoscience and Mineral Resources, 124 Gwahang-ro, Yuseong-gu, Daejeon 34132, Republic of Korea
[*]E-mail: skkim@kigam.re.kr (S. Kim), kfromberk@gmail.com (K. Kwon).

Received: 18 September 2015 / *Accepted:* 29 November 2015 / *Published:* 1 January 2016

A wide range of applications of room temperature ionic liquids (RTILs) in various fields inevitably require knowledge about their interaction with devices that are mainly composed of metallic materials. Degradation mechanism of metals and alloys in RTIL systems is supposed to be different from that in conventional aqueous system. We gathered some significant data from previously published papers to discuss a dissolution or passivation phenomenon that occurs on metallic electrodes in RTIL systems. The following two topics dominate literature on this field: corrosion behavior of metals and alloys in chloroaluminate RTILs, and anodic stability of aluminum in air- and water-stable RTILs. The composition ratio of constituted compounds is the main factor that determines the anodic stability of metal/alloys in the chloroaluminate RTILs, while the properties of surface layer formed by reactions between anions and metal ions are the crucial factor in the air- and water-stable RTIL systems.

Keywords: ionic liquid, corrosion, passivation, metal, alloy

1. INTRODUCTION

The term “room temperature ionic liquids (RTILs)”, which was coined in 1990s, refers to molten salts having a melting point below 100^{o}C [1]. RTILs have received immense attention because of their unique properties such as non/low-volatility and high ionic conductivity, differentiating themselves from other conventional liquids [2]. Meanwhile, almost unlimited variations of RTILs can be synthesized by combining numerous kinds of cations and anions. Therefore, it is possible to extract desirable properties for a specific application by designing RTILs properly. These features of RTILs have enabled the implementation of such advanced technologies, in which conventional aqueous or organic solvents cannot be used, as the electroplating of water-sensitive materials, the development of

low thermal runaway risk-batteries, and the dissolution of cellulose [3]. Along with the broadening of application of RTILs, one aspect that should be addressed is the stability or compatibility of materials in contact with applied RTILs. The interaction of RTILs with engineering materials is one of the key points to determine the viability of system to be implemented on an industrial scale.

Corrosion is a destructive result of chemical reaction between a metal or a metal alloy and its environment [4]. A corrosion process involves a transfer of electrons through anodic and cathodic reactions that occur simultaneously. The anodic reaction is the oxidation of metal while the cathodic reaction is the reduction of electrolytes or dissolved oxygen. In an aqueous system containing no oxygen, the reduction of water or hydrogen evolution occurs at cathodic sites. Metal ions resulting from the anodic reaction are surrounded by hydration layers and diffuse in the bulk aqueous electrolyte. On the other hand, the corrosion rate of some metals decreases at a certain potential that is sufficient for the formation of thin protective oxide film, which is known as passivation.

It is believed that an RTIL/metal interface is totally different from that between aqueous solution and metal. The large and asymmetrical ion structure of RTILs leads to a complex solvation behavior that can alter the solubility and diffusion properties of reactants. In RTILs composed of strongly coordinating anions such as bis(trifluoromethylsulfonyl)imide ($TFSI^-$) anion, a tight solvation layer is likely to form with dissolved metal ions, thus assisting metal dissolution. However, this phenomenon is unlikely to occur either in chloroaluminate RTILs or in RTILs with weakly coordinating anions such as tetrafluoroborate (BF_4^-) and hexafluorophosphate (PF_6^-) [5]. The lack of dissolved oxygen in RTIL systems also affects the corrosion mechanism of metals, generating consequently a different mechanism for passivation. One example is the RTIL/metal interface of lithium. Formation of a solid mixture of native surface film and anion reduction products [6], which is called solid electrolyte interphase (SEI), on Li metal immersed in TFSI-based RTILs is commonly observed. The SEI layer, which can permit the transfer of Li ions, could improve the electrochemical behavior of Li metal electrodes in rechargeable Li metal batteries. Furthermore, a surface layer that is intentionally preformed in RTIL solutions could inhibit the corrosion of metals applied in aqueous solutions. Pretreatment of reactive metals such as magnesium and its alloy in RTILs in order to form a protective surface film was proved to improve their corrosion resistance in NaCl solution [7].

Corrosion behavior of commonly applied metals and alloys in RTIL systems is an important topic as aforementioned. In particular, the anodic stability of metal and alloy components at a high potential plays a crucial role in the performance and the lifetime of devices for energy application. In spite of the fact that totally different corrosion and passivation mechanism from that of the conventional aqueous system is observed in RTIL systems, there is a limited knowledge of corrosion behavior of metallic materials in RTILs. Therefore, it would be meaningful at this present to collect and review relevant papers to the corrosion behavior of metals and alloys in various RTILs.

2. OVERVIEW OF METAL/ALLOY CORROSION IN RTILS

The corrosion behavior of metals depends on some factors such as kind of RTILs, temperature, impurities in RTILs and so on. For example, some commonly used metallic materials including nickel

and copper showed satisfying corrosion resistance in TFSI-based RTILs at room temperature [8,9]. Higher temperatures, however, could affect the corrosion behavior significantly, particularly on Cu, which showed six times higher corrosion current density at 70^{o}C than that at room temperature. Meanwhile, localized corrosion was detected on Ni, Inconel (Ni-chromium alloy), and carbon steel (CS) at 275^{o}C [8]. The corrosion of metals in RTILs is also affected by the presence of water. When 10 wt.% of water was added to an RTIL, the corrosivity of the resulting solution increased leading to a substantial increase in susceptibility to metal corrosion [10]. However, it has been claimed that traces of water in RTILs under aerobic conditions could inhibit the dissolution of Cu and Ni by accommodating a competitive anodic reaction, which is the oxidation of water to oxygen gas [11].

From an electrochemical point of view, potential is one of the most important factors determining the corrosion behavior in RTILs as well as the aforementioned factors. Because the corrosion behavior (dissolution/passivation) can be different at different potentials in the identical experimental conditions of RTIL, temperature and so on, it is difficult to generalize a specific trend in corrosion susceptibility of metallic materials. Therefore, we gathered available pieces of relevant information in literature and summarized them in terms of conditions where metallic materials show an active, passive, or active-to-passive transition behavior in various RTIL systems in Table 1, which could act as a guideline for material selection in RTIL systems. It was also found out from the summary that major efforts have been made either on metals in chloroaluminate RTILs or on Al metal in various RTILs. Therefore, we assign the following sections to each topic: firstly, on the corrosion behavior of several metallic materials in the chloroaluminate RTILs; and secondly, on the corrosion behavior of Al in air- and water-stable RTILs.

Table 1. Summary of metal/alloy corrosion behavior in RTILs in literature.

Metal / Alloy	**Corrosion behavior**	**Ref.**
Lewis acidic 1-butyl-3-methyl-imidazolium chloride – aluminum chloride (BMICl-$AlCl_3$)		
Ni	Active-to-passive transition. Passivation region in the potential range of 1.17 to 1.90 V vs. Ag (V_{Ag}).	12
Cu	Active dissolution without passivation.	
Ti	Passivation region in the potential range of 0.07 to 1.07 V_{Ag}.	
Lewis acidic 1-ethyl-3-methyl-imidazolium chloride – aluminum chloride (EMICl-$AlCl_3$)		
Ti	Active dissolution without passivation.	13
Mg	Active dissolution followed by the formation of viscous layer at a current density $\geq$ 5 mA/cm^2. Pit formation at a current density < 5 mA/cm^2.	14
Lewis neutral 1-ethyl-3-methyl-imidazolium chloride – aluminum chloride (EMICl-$AlCl_3$)		
Cu	Active dissolution without passivation.	15,16
Ni	Passivation region in the potential range of 1.0 to 2.6 V vs. Al (V_{Al}).	15,16
316 stainless steel (SS)	Active-to-passive transition. Passivation region in the potential range of 1.2 to 2.75 V_{Al}.	15

Ti	Active dissolution without passivation.	16,17
304 SS	Passivation region in the potential range of 1.1 to 3.2 V_{Al}.	16,17
CS	Active-to-passive transition. Passivation region in the potential range of 1.0 to 1.75 V_{Al}.	16,17
Mg	Passivation region at potentials above -1.8 V vs. Fc/Fc^+ (V_{Fc}).	16
Lewis basic 1-butyl-3-methyl-imidazolium chloride – aluminum chloride (EMICl-$AlCl_3$)		
Ni	Passivation region in the potential range of 0.24 to 1.14 V_{Ag}.	12
Cu	Active dissolution without passivation.	
Ti	Passivation region at potentials above 0.25 V_{Ag}.	
1-ethyl-3-methylimidazolium bis(trifluoromethylsulfonyl)imide (EMI-TFSI), 1-propyl-3-methylimidazolium bis(trifluoromethylsulfonyl)imide (PMI-TFSI), 1-butyl-3-methylimidazolium bis(trifluoromethylsulfonyl)imide (BMI-TFSI), 1-butyldimethylsulfonium bis(trifluoromethylsulfonyl)imide (S_{114}-TFSI)		
Al	Passive film formation at potentials above 5.0 V vs. Li (V_{Li}) due to the presence of protective Al-TFSI compound.	18,19
1-butyl-3-methylimidazolium tetrafluoroborate (BMI-BF_4)		
Al	Passive film formation at potentials above 5.0 V_{Li} due to the presence of protective AlF_3 compound.	19
trihexyl(tetradecyl)phosphonium bis(trifluoromethylsulfonyl)imide (P_{66614}-TFSI)		
Al	Passive film formation in the first cathodic scan and decreasing current density in the following cycles.	20
N-butyl-N-methylpyrrolidinium fluorosulfonyl(trifluoromethylsulfonyl)imide (BMP-FTFSI), N-butyl-N-methylpyrrolidinium bis(trifluoromethylsulfonyl)imide (BMP-TFSI)		
Al	Passive film formation at a potential of 5.0 V_{Li} and decreasing current density in the following cycles.	21,22
N-butyl-N-methylpyrrolidinium bis(fluorosulfonyl)imide (BMP-FSI)		
Al	Hysteresis and increasing current density from the second cycle, indicating Al dissolution.	22
N-methyl-N-propylpyrrolidinium bis(fluorosulfonyl)imide (PMP-FSI)		
Al	Increasing current density with cycling and larger reverse current than forward one, indicating pitting corrosion.	23
316 SS	Pit formation, selective oxidation of Fe and Ni at high potentials.	24
1-ethyl-3-methylimidazolium dicyanamide (EMI-DCA), N-butyl-3-methylpyrrolidinium dicyanamide (BMP-DCA)		
Ni, 304 SS, Ti, Al	Passivation behavior.	16
CS, Cu, Mg	Active dissolution without passivation.	
1-hexyl-3-methylimidazolium hexafluorophosphate (HMI-PF_6), 1-octyl-3-methylimidazolium hexafluorophosphate (OMI-PF_6), 1- butyl-3-methylimidazolium bis(trifluoromethanesulfonyl)imide (BMI-TFSI)		
CS	Active dissolution followed by weak passivation at high potentials.	25

1-butyl-3-methylimidazolium chloride (BMI-Cl)		
CS	Weak passivation followed by active dissolution at high potentials.	25
ethyl-dimethyl-propyl-ammonium bis(trifluoromethylsulphonyl)imide (EdMPN-TFSI)		
CS	Active-to-passive transition. Passivation region at potentials above 0.75 V vs. Pt (V_{Pt}).	26
304 SS	Passivation behavior at potentials above 0.00 V_{Pt}.	

3. METAL/ALLOY CORROSION IN CHLOROALUMINATE RTILS

Chloroaluminate RTIL is a first-generation ionic liquid that can be made by mixing aluminum Lewis acids and halide salts. The properties of this RTIL depend on its chloroacidity, which is determined by the mole fraction of aluminum Lewis acids in the mixture. Scheme 1 shows reaction series in three different natures of EMICl and $AlCl_3$ mixture. When the $AlCl_3$ mole fraction is less than 0.5, the melt could be categorized as basic due to an excess of Cl^- (Lewis base species). In the neutral melt (X ($AlCl_3$) = 0.5), all of the Cl^- anions are bound to Al^{3+} and the only species present is the $AlCl_4^-$ anion. When the mole fraction of $AlCl_3$ is greater than 0.5, the melt is considered as acidic due to the presence of $Al_2Cl_7^-$ species [27,28].

$$[EMI]^+Cl^- + AlCl_3 \leftrightarrow [EMI]^+[AlCl_4]^- \quad \text{(Neutral)}$$
$$[EMI]^+Cl^-_{excess} + AlCl_3 \leftrightarrow [EMI]^+[AlCl_4]^- + [EMI]^+Cl^- \quad \text{(Basic)}$$
$$[EMI]^+Cl^- + AlCl_{3_{excess}} \leftrightarrow [EMI]^+[AlCl_4]^- + AlCl_3 \leftrightarrow [EMI]^+[Al_2Cl_7]^- \quad \text{(Acidic)}$$

Scheme 1. Reaction series in the Lewis neutral, Lewis basic and Lewis acidic EMICl–$AlCl_3$ chloroaluminate RTILs.

This water-sensitive RTIL is quite promising as an electrolyte for electrodeposition of Al and Al alloys [29-35] as well as secondary batteries [36-38]. To check the compatibility of metallic materials with this RTIL, we collected the information on the corrosion behavior of commonly used metals, and confirmed that the chloroacidity of the RTIL most affects the corrosion behavior of applied metallic electrodes. We will discuss more details on the corrosion phenomena of metals and alloys observed in the acidic, neutral, and basic chloroaluminate RTILs in the following sections.

3.1. Lewis acidic chloroaluminate RTIL

Zhang et al. [12] observed an obvious active-to-passive transition behavior of Ni in acidic BMICl-$AlCl_3$. Anodic polarization of Ni electrode in this RTIL showed active dissolution followed by passivation in the potential range of 1.17 ~ 1.90 V_{Ag} and decomposition of the RTIL at ~2.00 V_{Ag}. Cu showed a completely different dissolution phenomenon from Ni in the same RTIL. Scanning electron microscope (SEM) examination of Cu surface after an anodic polarization test revealed a very rough

surface, which confirmed the general corrosion of Cu due to an attack of $Al_2Cl_7^-$ anion. In the case of titanium, a different corrosion behavior of Ti electrode was reported in acidic EMICl-$AlCl_3$ and BMICl-$AlCl_3$ RTILs. Approximately 1 V of passive potential range was observed in BMICl-$AlCl_3$ [12], while active dissolution without a passive potential region was observed in EMICl-$AlCl_3$ [13]. Zhang et al. suggested two plausible reasons for the different corrosion phenomena of Ti. The first is the effect of cation where different alkyl chains of ethyl and butyl affect the physicochemical properties of RTIL and induce different anodic polarization behavior. The second is the effect of electrode purity. The earlier study by Chen et al. [13] in EMICl-$AlCl_3$ used a commercially available Ti electrode (99.5%), while the following study by Zhang et al. [12] used a higher purity Ti (99.99%). A higher level of impurities that can dissolve immediately might create local anodic areas on the surface of the electrode, which induces Ti dissolution.

Porous oxide films on Mg surface are susceptible to dissolution in acidic EMICl-$AlCl_3$. Initial breakdown of thinner parts of the oxide film allows the dissolution of Mg into the bulk RTIL. Viscosity of EMICl-$AlCl_3$ linearly increased with increasing dissolved Mg content [39]. At some point, the viscosity of the RTIL is high enough to retard the diffusion process of freshly oxidized Mg^{2+} into the bulk RTIL. Therefore, the accumulation of Mg^{2+} at an electrode interface occurred and resulted in the formation of a viscous layer in galvanostatic anodic polarization at high current density ($\geq$ 5 mA/cm^2) [14]. The absence of pits observed on the Mg surface after the anodic polarization confirmed that the Mg electrode was homogenously dissolved into the RTIL. On the contrary, the anodic polarization at a lower current density led to local pit formation without the generation of a viscous layer. This is because the dissolution process was not rapid and hence the Mg dissolution only occurred locally at the initially-broken thinner parts of the oxide film.

3.2 Lewis neutral chloroaluminate RTIL

A polarization test of Cu electrode in Lewis neutral EMICl-$AlCl_3$ showed completely active dissolution with a limiting current density of approximately 40 mA/cm^2, as shown in Figure 1 (curve b) [15]. Energy-dispersive X-ray spectrometer (EDS) analysis after the polarization test confirmed that no other elements than Cu were detected on the roughened electrode surface, suggesting that the formation of Cu complex ions might be a reason for Cu dissolution in Lewis neutral EMICl-$AlCl_3$. Similarly, the formation of Ti complex ions such as $Ti(AlCl_4^-)_x^{(x-n)^-}$ in Lewis neutral EMICl-$AlCl_3$ has also been suggested as a cause of rapid current increase in the anodic polarization of the Ti electrode [17]. On the other hand, Ni has been reported to have good corrosion resistance in Lewis neutral EMICl-$AlCl_3$ [15]. No evidence of corrosion such as pit formation on Ni surfaces observed from SEM micrographs indicated that a transpassive current measured at potentials higher than 2.6 V_{Al} in Figure 1 (curve a) was attributed not to the corrosion of the Ni electrode but to the oxidation of the RTIL species ($4AlCl_4^- \rightarrow 2Al_2Cl_7^- + Cl_2 + 2e^-$). In contrast with the anodic polarization behavior of Mg in Lewis acidic EMICl-$AlCl_3$, Mg electrodes exhibited a wide passivation region in the Lewis neutral one. The Mg electrode surfaces remained intact after being potentiostatically etched at -0.5 V_{Fc}

for 1 h, which confirmed an unconventional passivation phenomenon of Mg in Lewis neutral EMICl-$AlCl_3$ [16].

Two types of stainless steel, 316 SS and 304 SS, revealed a different polarization behavior in Lewis neutral EMICl-$AlCl_3$. An active-to-passive transition behavior was observed on 316 SS while a prominent passivation behavior with a very wide potential range (from 1.1 to 3.2 V_{Al}) was observed on 304 SS [15,17]. In the case of 316 SS (Figure 1, curve c), the current density increased to 0.2 mA/cm^2 as potential anodically increased from the corrosion potential (0.6 V_{Al}) to 1.2 V_{Al}, and then started to decrease. At 1.9 V_{Al}, a little bump was observed and indicated a slight increase of current that might be attributed to further oxidation of passive films. Meanwhile, carbon steel showed a similar active-to-passive transition to 316 SS at around 1.0 V_{Al} in Lewis neutral EMICl-$AlCl_3$ [17]. However, the passivation mechanism in this RTIL was not clearly revealed because no evidence of passive layer formation was found by both SEM and EDS analyses after potential was held in the passivation region (1.5 V_{Al}) for 30 min.

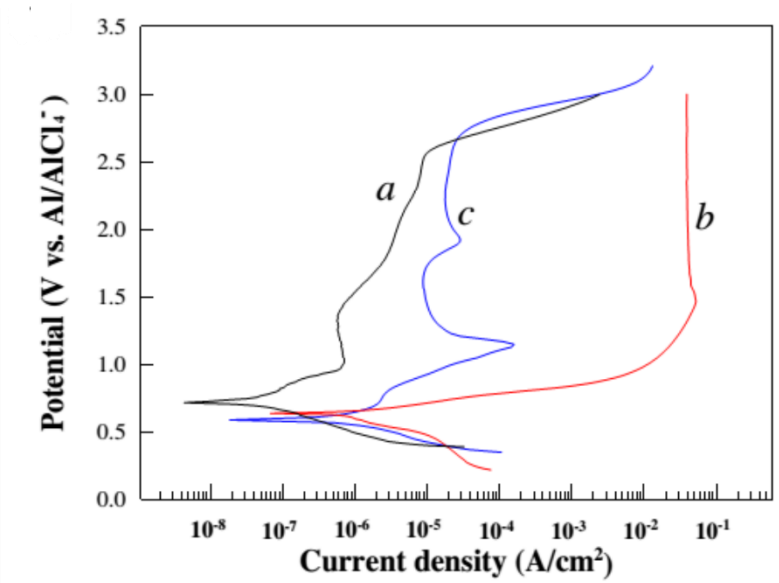

Figure 1. Polarization curves of Ni (curve a), Cu (curve b), and 316 SS (curve c) measured in Lewis neutral EMICl-$AlCl_3$ (Reprinted with permission from ref. [15]. Copyright 2011, Elsevier B.V).

3.3 Lewis basic chloroaluminate RTIL

To our knowledge, only one paper that performed corrosion of metals in Lewis basic chloroaluminate RTIL has been published so far. Zhang et al. [12] examined the corrosion behaviors of Ni, Ti and Cu in this RTIL. Different from the anodic polarization behavior in acidic BMICl-$AlCl_3$, Ni showed a passive behavior that extended from above a corrosion potential to 1.14 V_{Ag} and was followed by a transpassive behavior at higher potentials in basic BMICl-$AlCl_3$. In the case of Cu, pitting corrosion occurred such that 5 μm pits appeared on a Cu electrode surface after an anodic polarization test, confirming that Cu suffers corrosion in the basic BMICl-$AlCl_3$ in a different

mechanism from the acidic one where the general corrosion was observed. By contrast, Ti showed a passive behavior in the basic BMICl-$AlCl_3$ similar with the acidic one except showing a higher current density and a higher corrosion potential. Breakdown potential was not observed in the studied potential range (up to 2 V_{Ag}), which confirmed the excellent stability of a passive film formed on the Ti surface in this RTIL.

Because Cu is the most susceptible to corrosion in the presence of chloroaluminate RTILs among the investigated metals, it might be worthwhile to summarize the corrosion behavior of Cu as follows. Cu does not seem appropriate to be used in all types of chloroaluminate RTILs considering that active dissolution was observed in all tested chloroaluminate RTILs. However, different corrosion mechanism can occur in the basic one where local pits were observed only in this case. This may be due to the presence of Cl^- species, which induce pit formation on the Cu surface in the basic chloroaluminate RTILs. On the other hand, $AlCl_4^-$ and $Al_2Cl_7^-$ anions are likely to form complex ions with Cu^{2+} that are soluble in the chloroaluminate RTILs so that massive dissolution of Cu was favored in both Lewis neutral and Lewis acidic chloroaluminate RTILs. SEM images shown in Figure 2 confirm a distinct appearance of Cu electrodes after polarization tests in the Lewis neutral, Lewis acidic, and Lewis basic chloroaluminate RTILs.

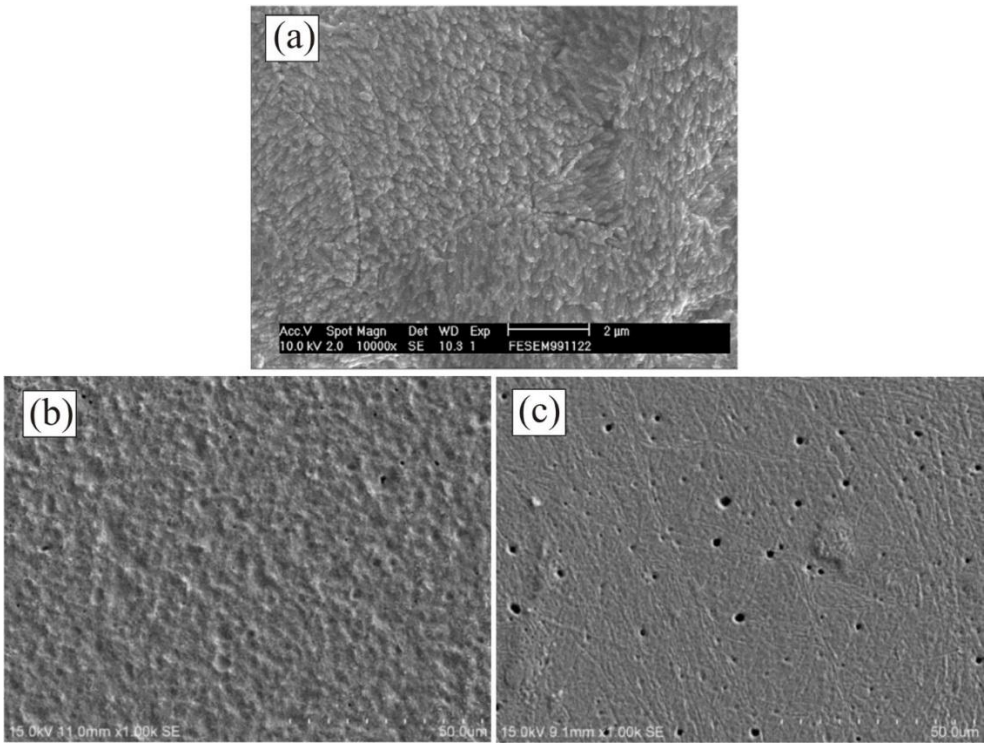

Figure 2. SEM images of Cu electrode surface after anodic polarization in Lewis neutral EMICl-$AlCl_3$ (a) (Reprinted with permission from ref. [15]. Copyright 2011, Elsevier B.V), Lewis acidic BMICl-$AlCl_3$ (b) and Lewis basic BMICl-$AlCl_3$ (c) [12].

4. ALUMINUM CORROSION IN AIR- AND WATER-STABLE RTILS

The air- and water-stable RTILs, composed of hydrophobic anions, are considered as the second generation of RTILs. Theoretically, 10^{18} kinds of air- and water-stable RTILs are possible to be

synthesized [40], and hence they are likely to dominate the electrochemistry field in the near future. This type of RTILs is promising to be applied in lithium-ion battery (LIB) applications due to their excellent electrochemical stability as well as low volatility and non-flammability compared to conventional aprotic organic solvents. Even though commercial application of LIB utilizing RTIL has not been established yet [41], extensive study of air- and water-stable RTILs in LIB application is continuously growing.

As for now, Al is the most suitable metal to be used as a positive electrode current collector for LIB due to its low cost, high conductivity as well as stability in most electrolytes studied [42]. Generally, a thin protective film would be formed on the surface of Al current collector as a reaction product between Al cation and anion species from salts or solvents. However, not every reaction product formed is insoluble in electrolytes. Thus, the Al current collector may encounter dissolution if a reaction product is soluble, and the resulting Al corrosion incurs the deterioration of battery performance. Significant results of Al current collector anodic behavior that have been obtained so far in several kinds of RTILs will be discussed here in regard to the effect of alkyl chain length in cation part and properties of surface layer formed by anions.

4.1. The effect of cations

Peng et al. [18,19] investigated the anodic polarization behavior of Al foils in TFSI-based RTILs. The shape of cyclic voltammogram (CV) of Al foil electrodes in EMI-TFSI, PMI-TFSI, and BMI-TFSI containing lithium-TFSI salt (LiTFSI) was similar, which suggested the anodic behavior of the Al foil electrodes in these RTILs are principally the same. At a potential between 2.8 and 3.5 V_{Li}, an anodic current initiated and gradually increased until potential was reversed at 5.0 V_{Li} in the first cycle. The absence of anodic current in the following cycles suggested that passivation occurred, and thus the RTILs remained stable up to potential about 5.0 V_{Li}. However, the potential values where the anodic current started to develop in the first cycle were slightly different for the three RTILs, which showed an increasing tendency as the alkyl chain in the cations became longer. It could be assumed from these results that a longer alkyl chain has a tendency to widen a potential window although it does not affect the overall cycling performance once the passivation has occurred. Fourier transformed infrared spectroscopy and EDS spectra of Al foil electrodes after the CV measurements in these RTILs showed the existence of elements from $TFSI^-$ in addition to Al, and it was concluded that Al-TFSI compound formed and acted as a protective film on the Al electrode surface to prevent Al dissolution at high potentials.

The formation of protective films on Al foil electrodes was also confirmed in sulfonium- and phosphonium-based RTILs with the same $TFSI^-$ anion. CV measurements in S_{114}-TFSI [19] and P_{66614}-TFSI [20] containing 1 M LiTFSI salt exhibited passive layer formation on Al foil electrode surface on the first scan, and further oxidation was suppressed in the following cycles due to the resistance of the passive layer as shown in Figure 3 for the P_{66614}-TFSI case.

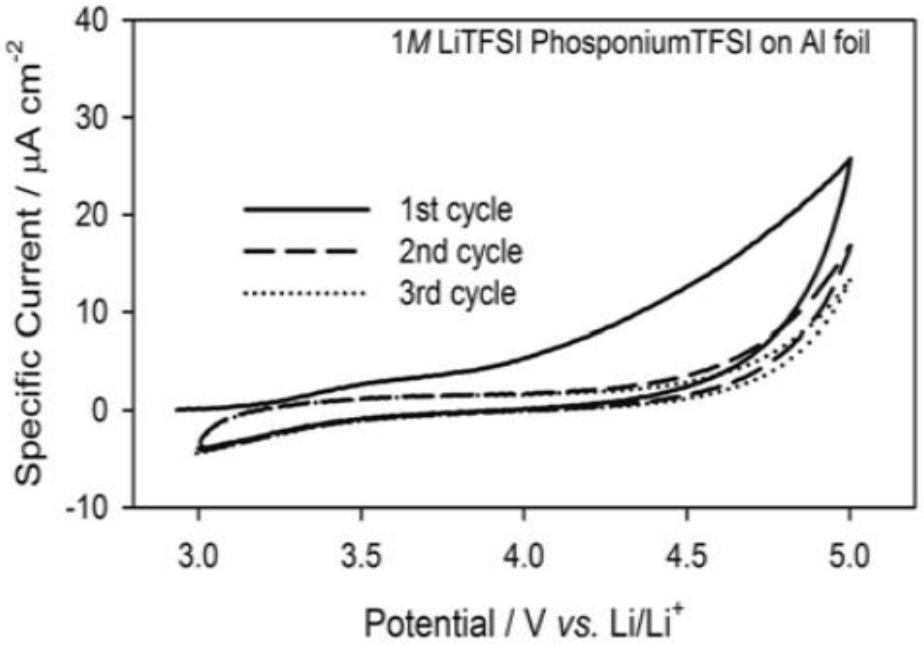

Figure 3. CV curve of Al foil electrode in P_{66614}-TFSI containing 1 M LiTFSI salt (Reprinted with permission from ref. [20]. Copyright 2011, KECS).

4.2. The effect of anions

Anion is known to have a major effect on the stability of Al electrodes in RTILs. Oxidation products formed by reactions between anion species and Al cations are strongly related to the anodic behavior of Al electrode. EDS and X-ray photoelectron spectroscopy of Al electrode surface after an anodic potentiostatic experiment in LiTFSI-containing BMI-TFSI at 4.2 V_{Li} for 3 h confirmed the presence of Al-TFSI compound as a main component of protective layers. In the case of BMI-BF_4 containing $LiBF_4$ salt, AlF_3 and Al_2O_3 were observed deposit on Al electrode surface after a potential was held at the same value of 4.2 V_{Li} contrary to the expectation that Al-BF_4 would be formed as an oxidation product [19]. This result may be attributed to different anodic behavior of BF_4^- from $TFSI^-$ such that the BF_4^- anion might be oxidized at the applied potential and release free fluorine species that react with the Al cations and then form AlF_3 compounds. Meanwhile, the observed Al_2O_3 after the anodic potentiostatic experiment might originate from the existing Al_2O_3, which was not completely removed after a cleansing process, on the Al surface before the experiment considering the lack of oxygen sources in the experiment environment.

Beside the $TFSI^-$ anion, other types of [(perfluoroalkyl)sulfonyl]imide anions that have been studied frequently in LIB and supercapacitor applications are FSI^- and $FTFSI^-$ with structures shown in Figure 4. It is known that the properties of RTILs consisting of pyrrolidinium-based cations and $FTFSI^-$ anions such as thermal stability and conductivity are in between pyrrolidinium-based RTILs with $TFSI^-$ and FSI^- anions [21]. In terms of anodic stability of Al electrodes in the three RTILs (note CVs in Figure 5), BMP-FTFSI exhibited a similar response to BMP-TFSI, which showed a typical passivation behavior such that anodic currents keep decreasing in the following cycles [21,22]. CV

curve shape was different for BMP-FSI, which showed increasing anodic currents with cycling as well as hysteresis after the second cycle indicative of Al dissolution. As aforementioned, the formation of complex Al-anion compounds can occur in these RTILs. However, a generated Al-FSI film is considered to be less dense compared to Al-FTFSI and Al-TFSI. Hence, some fragile spots could be oxidized during the oxidation scan in the second cycle, which triggers pit formation.

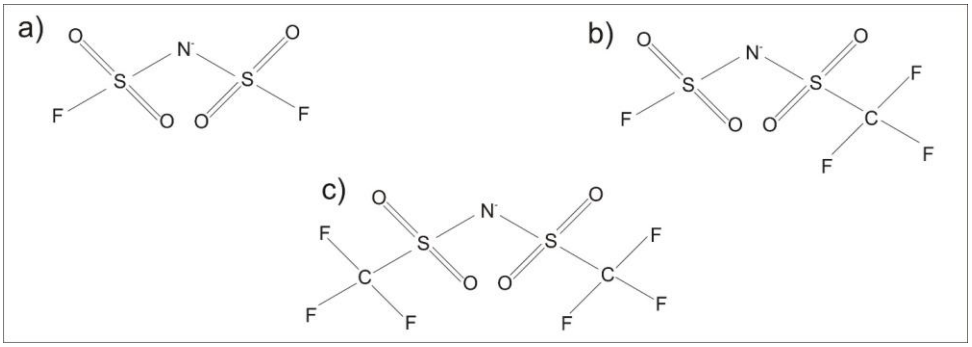

Figure 4. Schematic structures of FSI^- (a), $FTFSI^-$ (b) and $TFSI^-$ (c) anions.

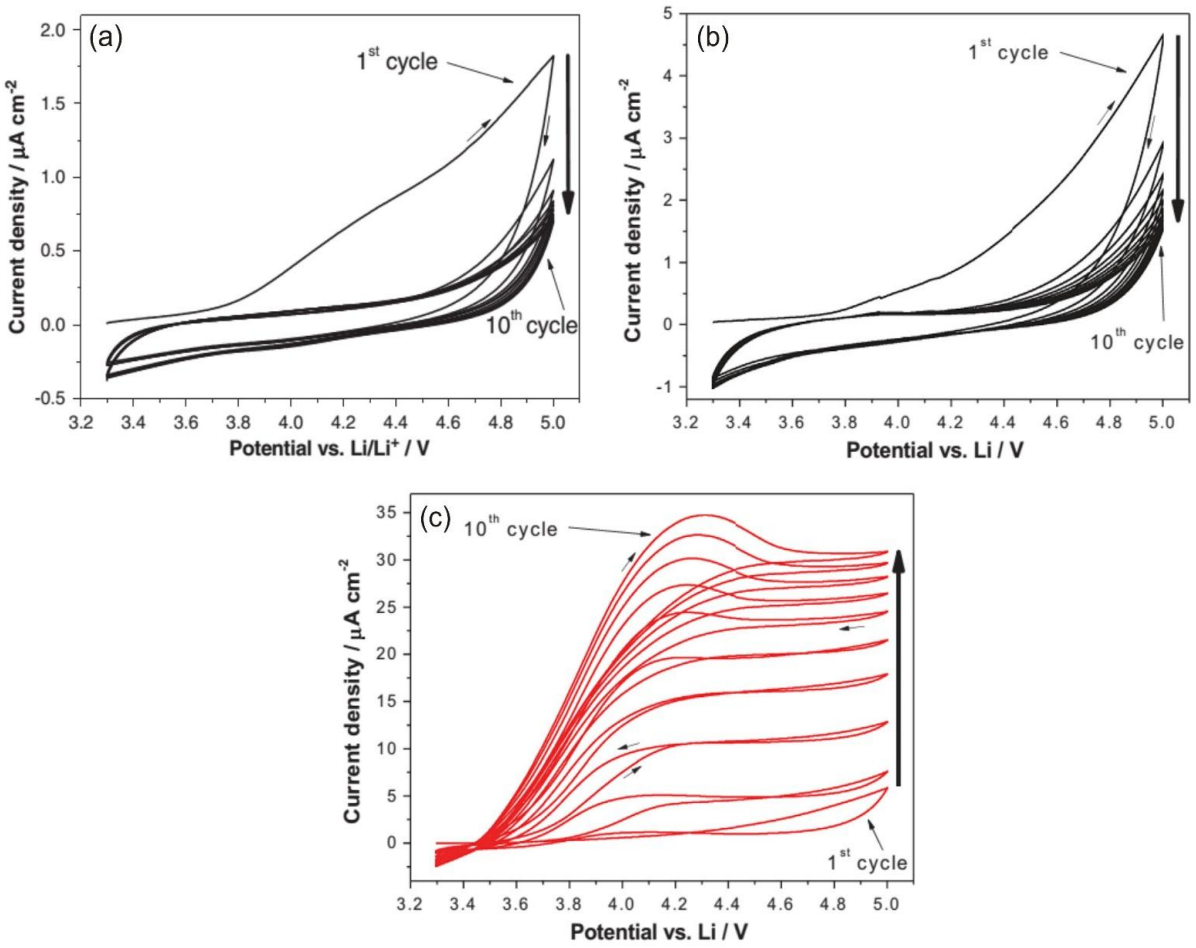

Figure 5. CV curves of Al electrodes in BMP-FTFSI (a) (Reprinted with permission from ref. [21]. Copyright 2013, Elsevier B.V), BMP-TFSI (b) and BMP-FSI (c) (Reprinted with permission from ref. [22]. Copyright 2014, Elsevier B.V).

The increasing current response in the following cycles indicated continuous dissolution on pits. It was confirmed by SEM images that some dark pits appeared on the Al electrode surface after the CV measurement in BMP-FSI, while it remained intact in BMP-FTFSI and BMP-TFSI. The reason behind the different nature of the films is still unknown, but a higher diffusion coefficient of FSI^- than $FTFSI^-$ and $TFSI^-$ due to a different ion size [43] could affect the nature of the film. Therefore, the Al-FSI compound is more subject to dissolution into the electrolyte, which makes the film less compact.

Cho et al. found that pitting corrosion of Al electrode occurred in PMP-FSI from a CV showing a gradual increase in current with cycles and a larger reverse current than the forward one [23]. Anodic polarization at above 4.0 V_{Li} resulted in pitting formation, which is assumed to be due to the dissolution of Al-FSI compound at some local points. However, the pitting corrosion could be suppressed by an addition of $LiPF_6$ salt to the electrolyte. A passivation layer consisting of AlF_3 compound was generated instead of Al-FSI [44], and it was confirmed that complete passivation was obtained in the $LiPF_6$-added electrolyte. Similar pitting corrosion phenomenon also occurred on 316 SS, a common casing material used in coin-type cells for LIB, during electrochemical tests in the same RTIL [24]. Selective oxidation of iron and nickel from 316 SS followed by solvation of oxidized ions by the RTIL was observed, leaving considerable pits on the 316 SS electrode surface.

5. CONCLUSIONS

We reviewed anodic behavior of some metallic materials in the chloroaluminate RTILs as well as in the air- and water-stable RTILs from previous studies that have been published so far. We can concluded that chloroacidity is the main factor determining the anodic behavior in the former type of RTILs, whereas the length of alkyl chain in cations and the properties of surface layer formed by reaction between anions and metal ions are the main factor in the latter ones. It is clearly different from corrosion in common aqueous system, which is dominantly affected by concentration of hydrogen ions and dissolved oxygen.

In the Lewis acidic chloroaluminate RTILs, metallic electrodes tend to be actively dissolved due to the formation of complex compounds with excess $Al_2Cl_7^-$ anions. Cu exhibited incompatibility in all nature of chloroaluminate RTILs, and hence it is recommended to avoid the application of Cu in this system. The surprisingly unconventional passivation of Mg that was observed in Lewis neutral EMICl-$AlCl_3$ needs to be further investigated to find out the passivation mechanism of Mg in the RTIL system.

In the air- and water-stable RTILs, an anodic stability limit is affected by cation type. A longer alkyl chain gives a higher limit. The tendency of complex compound formation between metal ions and the anions of RTIL electrolytes was also found in the air- and water-stable RTIL systems. Depending on anion types, metal dissolution or formation of protective surface layer could occur in the RTIL systems. The metal electrode stability in cycling depends on the properties of the surface layer such that compact surface layer could act as a barrier for further metal dissolution. The TFSI-based RTILs are likely to be compatible with Al electrodes, due to the passivation behavior observed with various types of cations.

ACKNOWLEDGEMENT
This study was supported by the R&D Center for Valuable Recycling (Global-Top Environment Technology Development Program) funded by the Ministry of Environment (Project No.: GT-14-C-01-036-0).

References

1. K.N. Marsh, J.A. Boxall and R. Lichtenthaler, *Fluid Phase Equilib.*, 219 (2004) 93.
2. H. Ohno, *Electrochemical Aspects of Ionic Liquids*, John Wiley & Sons, Inc., 2005, Ch.1.
3. M. Armand, F. Endres, D. R. MacFarlane, H. Ohno and B. Scrosati, *Nat. Mater.*, 8 (2009) 621.
4. Jones, D. A., *Principles and Prevention of Corrosion*, Macmillan, 1992, Ch.1.
5. Y. Z. Su, Y. C. Fu, Y. M. Wei, J. W. Yan and B. W. Mao, *ChemPhysChem*, 11 (2010) 2764.
6. P. C. Howlett, N. Brack, A. F. Hollenkamp, M. Forsyth and D. R. Macfarlane, *J. Electrochem. Soc.*, 153 (2006) A595.
7. P. Huang, J. A. Latham, D. R. MacFarlane, P. C. Howlett and M. Forsyth, *Electrochim. Acta*, 110 (2013) 501.
8. I. Perissi, U. Bardi, S. Caporali and A. Lavacchi, *Corros. Sci*., 48 (2006) 2349.
9. I. Perissi, S. Caporali, A. Fossati and A. Lavacchi, *Advances in Chemistry Research Volume 6*, Nova Science Publisher, 2011, Ch.12.
10. M. Uerdingen, C. Treber, M. Balser, G. Schmitt and C. Werner, *Green Chem.*, 7 (2005) 321.
11. O. Lebedeva, G. Jungurova, A. Zakharov, D. Kultin, E. Chernikova and L. Kustov, *J. Phys. Chem. C*, 116 (2012), 22526.
12. Q. Zhang, Y. Hua and Z. Zhou, *Int. J. Electrochem. Sci.*, 8 (2013) 10239.
13. J. R. Chen, W. T. Tsai and I. W. Sun, *J. Electrochem. Soc.*, 159 (2012) C298.
14. B. Xu, R. Qu and G. Ling, *Electrochim. Acta*, 149 (2014) 300.
15. P. C. Lin, I. W. Sun, J. K. Chang, C. J. Su and J. C. Lin, *Corros. Sci*., 53 (2011) 4318.
16. Y. C. Wang, T. C. Lee, J. Y. Lin, J. K. Chang and C. M. Tseng, *Corros. Sci.*, 78 (2014) 81.
17. C. H. Tseng, J. K. Chang, J. R. Chen, W.T. Tsai, M. J. Deng and I. W. Sun, *Electrochem. Commun.*, 12 (2010) 1091.
18. C. Peng, L. Yang, Z. Zhang, K. Tachibana and Y. Yang, *J. Power Sources*, 173 (2007) 510.
19. C. Peng, L. Yang, Z. Zhang, K. Tachibana, Y. Yang and S. Zhao, *Electrochim. Acta*, 53 (2008) 4764.
20. E. Cha, J. Mun, E. Cho, T. Yim, Y. G. Kim, S. M. Oh, S. A. Lim and J. W. Lim, *J. Korean Electrochem. Soc.*, 14 (2011) 152.
21. R-S. Kühnel, J. Reiter, S. Jeong, S. Passerini and A. Balducci, *Electrochem. Commun.*, 38 (2014) 117.
22. R-S. Kühnel and A. Balducci, *J. Power Sources*, 249 (2014) 163.
23. E. Cho, J. Mun, O. B. Chae, O. M. Kwon, H. T. Kim, J. H. Ryu, Y. G. Kim and S. M. Oh, *Electrochem. Commun.*, 22 (2012) 1.
24. T. Evans, J. Olson, V. Bhat and S. H. Lee, *J. Power Sources*, 269 (2014) 616.
25. M. F. Arenas and R. G. Reddy, *J. Min. Metall. Sect. B-Metall*., 39 (2003) 81.
26. I. Perissi, U. Bardi, S. Caporali, A. Fossati and A. Lavacchi, *Sol. Energy Mater. Sol. Cells*, 92 (2008) 510.
27. T. J. Melton, J. Joyce, J. T. Maloy, J. A. Boon and J. S. Wilkes, *J. Electrochem. Soc.*, 137 (1990) 3865.
28. T. Welton, *Chem. Rev*., 99 (1999) 2071.
29. M. Zhang, J. S. Watson, R. M. Counce, P. C. Trulove and T. A. Zawodzinski Jr., *J. Electrochem. Soc.*, 161 (2014) D163.
30. T. Jiang, M. J. C. Brym, G. Dubé, A. Lasia and G. M. Brisard, *Surf. Coat. Technol*., 201 (2006) 1.
31. T. Tsuda, Y. Ikeda, T. Arimura, M. Hirogaki, A. Imanishi, S. Kuwabata, G. R. Stafford and C. L. Hussey, *J. Electrochem. Soc.*, 161 (2014) D405.
32. Y. Zheng, S. Zhang, X. Lu, Q. Wang, Y. Zuo and L. Liu, *Chin. J. Chem. Eng.*, 20 (2012) 130.

33. Q. X. Liu, S. Z. El Abedin and F. Endres, *Surf. Coat. Technol*., 201 (2006) 1352.
34. J. K. Chang, S. Y. Chen, W. T. Tsai, M. J. Deng and I. W. Sun, *Electrochem. Commun.*, 9 (2007) 1602.
35. S. J. Pan, W. T. Tsai, J. K. Chang and I. W. Sun, *Electrochim. Acta*, 55 (2010) 2158.
36. B. Vestergaard, N. J. Bjerrum, I. Petrushina, H. A. Hjuler, R. W. Berg and M. Begtrup, *J. Electrochem. Soc*., 140 (1993) 3108.
37. J. J. Auborn and Y. L.Barberio, *J. Electrochem. Soc.*, 132 (1985) 598.
38. R. Revel, T. Audichon and S. Gonzalez, *J. Power Sources*, 272 (2014) 415.
39. B. Xu, J. Chen and G. Ling, *Electrochem. Solid-State Lett*., 15 (2012) D1.
40. F. Endres and S. Z. El Abedin, *Phys. Chem. Chem. Phys*., 8 (2006) 2101.
41. A. H. Whitehead and M. Schreiber, *J. Electrochem. Soc.*, 152 (2005) A2105.
42. D. R. MacFarlane, N. Tachikawa, M. Forsyth, J. M. Pringle, P. C. Howlett, G. D. Elliott, J. H. Davis, Jr., M. Watanabe, P. Simon and C. A. Angell, *Energy Environ. Sci.*, 7 (2014) 232.
43. J. Reiter, S. Jeremias, E. Paillard, M Winter and S. Passerini, *Phys. Chem. Chem. Phys*., 15 (2013) 2565.
44. M. Morita, T. Shibata, N. Yoshimoto and M. Ishikawa, *Electrochim. Acta*, 47 (2002) 2787.